Numerical and experimental investigation of a continuous-wave and passively mode-locked Yb:YAG laser at a wavelength of 1.05 μm

Binbin Zhou,[1] Zhiyi Wei,[1,*] Dehua Li,[1] Hao Teng,[1] and Gilbert L. Bourdet[2]

[1]Laboratory of Optical Physics, Institute of Physics, Chinese Academy of Sciences, Beijing 100190, China

[2]LULI , UMR 7605, CNRS-CEA-Ecole Polytechnique-Paris VI, Ecole Polytechnique, 91128 Palaiseau Cedex, France

*Corresponding author: zywei@aphy.iphy.ac.cn

Received 13 March 2009; revised 4 September 2009; accepted 12 October 2009; posted 12 October 2009 (Doc. ID 108657); published 26 October 2009

We present the results of a novel numerical and experimental investigation aimed at obtaining efficient 1.05 μm operation with a Yb:YAG laser. The model shows that the emitting wavelength of the Yb:YAG laser is affected by the combination of length and doping concentration of the gain medium. Efficient continuous-wave laser operation at the wavelength of 1050 nm was experimentally obtained in good agreement with the model predictions. Based on continuous-wave operation, generation of 1.8 ps laser pulses at the central wavelength of 1050 nm, as well as 170 fs laser pulses at the central wavelength of 1053 nm, were realized.

OCIS codes: 140.3580, 140.3615, 140.4050, 140.7090.

1. Introduction

Passive mode locking of diode-pumped ytterbium-doped lasers by semiconductor saturable absorber mirrors (SESAMs) has become a standard way to obtain ultrafast pulses in the 1 μm wavelength region. Among a variety of Yb-doped crystals, the Yb:YAG crystal is one of the most important laser mediums for this application for several important advantages: excellent thermal–mechanical properties, ease of growth in high-quality crystal, and a high doping concentration without quenching. Because of these favorable properties, remarkable progress has been achieved with ultrashort Yb:YAG oscillators. An average output power as high as 80 W [1] and a pulse energy higher than 10 μJ [2,3] at a wavelength of 1030 nm have been demonstrated. Typically, the Yb:YAG crystal has two main emission wavelengths, 1.03 and 1.05 μm. An ultrafast Yb:YAG laser operating at 1.05 μm has special advantages in comparison with a laser at 1.03 μm. First, the gain around 1.05 μm is flatter and can support femtosecond pulses with a broader spectrum and shorter pulse width. Yb:YAG laser pulses as short as 100 fs have been demonstrated at this wavelength [4]. In contrast, limited by the width of the narrow gain peak at 1030 nm, the shortest pulse achieved at this wavelength has a width of 340 fs [5], and most femtosecond pulses are longer than 500 fs [1–3,6–8]. Second, ultrashort pulses at 1.05 μm can be useful in large glass laser facilities as the seeding source.

To obtain oscillation at 1.05 μm by the Yb:YAG laser, one must suppress the oscillation at 1030 nm. Some studies have been reported about specially coated mirrors to distinguish these two neighboring wavelengths [5,9], which, however, inevitably brings additional cavity losses and leads to low laser efficiency. Wavelength control has already been intensively studied in ytterbium-doped silica fiber lasers [10,11]. However, to the best of our knowledge, there are no published results about the relationship between the emission wavelength and the parameters of the gain medium in a solid-state Yb:YAG laser. We

0003-6935/09/315978-06$15.00/0

investigated the preferred emission wavelength versus the length and the ion concentration of the Yb:YAG crystal theoretically and developed a novel method to obtain efficient 1050 nm operation based on the Yb:YAG laser. On this basis, we obtained 170 fs laser pulses at the central wavelength of 1053 nm.

2. Theoretical Investigation

The electronic diagram of a ytterbium ion is shown in Fig. 1; it is a typical quasi-three-level system. As the zero phonon line is very narrow and the corresponding absorption cross section is lower, the most efficient pump transition for Yb:YAG is l_1 to u_2 at 940 nm. Emission transitions are from u_1 to l_2 (1024 nm) to l_3 (1030 nm) to l_4 (1050 nm). For a quasi-three-level longitudinally pumped laser system, the thickness of the gain medium is more crucial for the laser oscillation than in a four-level system. In a quasi-three-level system, the terminal level of the laser transition is thermally populated. Thus minimum pump intensity is required to reach population inversion. As the pump is absorbed when it travels in the gain medium, this minimum intensity is reached after a crystal length, which is the so-called optimum length. In the following we investigate the different optimum lengths at different oscillation wavelengths in a Yb:YAG laser by the model developed in [12,13].

Amplification of the laser wave and the absorption of the pump wave are described by

$$\frac{dI_l^{\varepsilon}}{I_l^{\varepsilon}} = \varepsilon g_0 \{X_u - f_l\} dz, \tag{1a}$$

$$\frac{dI_p^{\varepsilon'}}{I_p^{\varepsilon'}} = -\varepsilon' \alpha_0 \{f_p - X_u\} dz, \tag{1b}$$

where X_u is the population density of the excited state, $X_u = N_u/N_{\mathrm{Yb}}$, N_u is the population of the excited state, and N_{Yb} is the Yb^{3+} ion concentration. The linear coefficients of gain g_0 and absorption α_0 are given by

$$g_0 = \sigma_l N_{\mathrm{Yb}}(f_{lk} + f_{u1}), \qquad \alpha_0 = \sigma_p N_{\mathrm{Yb}}(f_{l1} + f_{uj}), \tag{2}$$

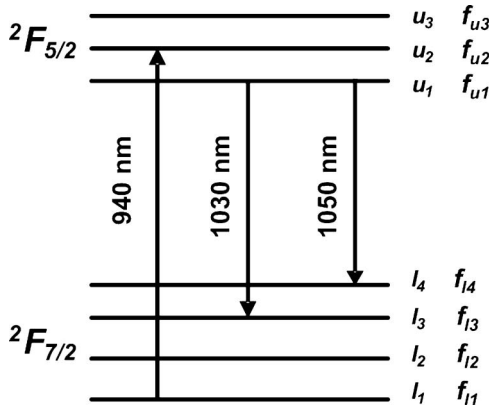

Fig. 1. Energy level diagram of Yb^{3+} ion in the Yb:YAG crystal.

with

$$f_l = \frac{f_{lk}}{f_{lk} + f_{u1}}, \qquad f_p = \frac{f_{l1}}{f_{l1} + f_{uj}},$$

where σ_p and σ_1 are the absorption and emission cross sections and f_{jk} represents the Boltzmann partition factors of sublevel k of manifold j, and ε and ε' are ± 1 relative to the direction of propagation of the laser and the pump beams, respectively. The dynamic equation for the population reads as

$$\tau_u \frac{dX_u}{dt} = I_p(f_p - X_u) - X_u - I_l(X_u - f_l), \tag{3}$$

where τ_u is the excited-state lifetime and I_p and I_l are the pump and laser intensity that travel in both directions normalized to the saturation intensity given by

$$I_{\mathrm{sat}}^{l} = \frac{h\nu_l}{(f_{lk} + f_{u1})\tau_u \sigma_l}, \qquad I_{\mathrm{sat}}^{p} = \frac{h\nu_p}{(f_{l1} + f_{uj})\tau_u \sigma_p}. \tag{4}$$

In the continuous-wave regime, Eq. (3) reads as

$$I_p(f_p - X_u) - X_u - I_l(X_u - f_l) = 0.$$

Then

$$X_u = \frac{f_p I_p + f_l I_l}{1 + I_p + I_l}, \qquad I_i = I_i^{+} + I_i^{-}. \tag{5}$$

With regard to Eq. (1a), the laser beam is reabsorbed when $X_u < f_l$. Then the minimum pump intensity required to bleach the amplifier medium is given by

$$X_u = f_l, \qquad I_p^{\min} = \frac{f_l}{f_p - f_l}. \tag{6}$$

We now consider single-pass pumping when the pump travels in one direction. For single-pass pumping, the pump transmission required to invert the amplifier medium is given by

$$I_p(0)\Gamma = I_p^{\min}, \qquad \Gamma = \beta = \frac{I_p^{\min}}{I_p(0)}. \tag{7}$$

As the pump is absorbed when it travels in the amplifier, this minimum intensity required to bleach the amplifier medium at the laser wavelength is reached

Table 1. Values of the Crystal Parameters

Parameters	Absorption	Emission	
λ(nm)	940	1030	1050
$f_u + f_l$	1.04E + 00	0.75	7.00E-01
σ(cm^2)	7.60E-21	3.30E-20	4.80E-21
τ_u(ms)	0.95	0.95	0.95
f_i	0.838	0.0626	0.0205

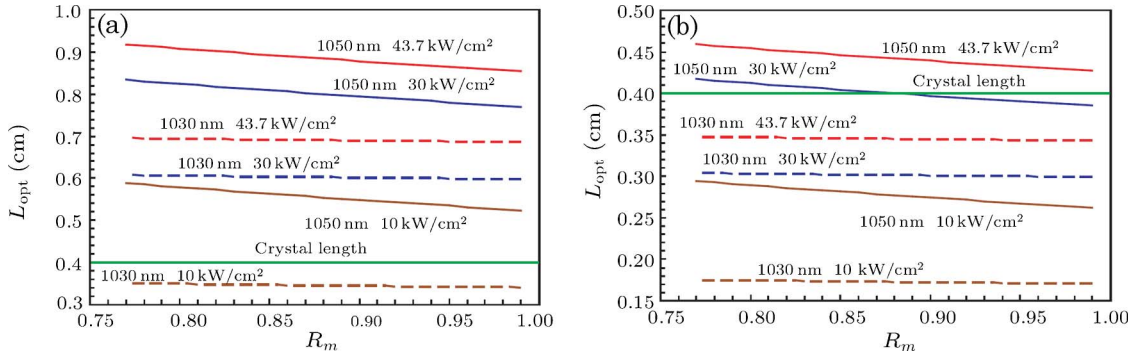

Fig. 2. (Color online) Optimum length versus reflectivity of the rear mirror for various pump intensities with (a) 5% and (b) 10% doping.

after an amplifier length we call optimum length. For single-pass pumping and a continuous-wave laser, the output intensity has been derived in [13]:

$$I_{\text{out}}(L) = (1-R_s)\sqrt{R_m}\,\frac{g_0\left(\frac{I_p(0)(1-\Gamma)}{\alpha_0} - f_l L\right) + \ln\sqrt{R_m R_s}}{(1-\sqrt{R_m R_s})(\sqrt{R_m}+\sqrt{R_s})}, \tag{8}$$

where R_s and R_m are the reflectivity of the output and rear mirrors, respectively (in our case, we assume that all the losses of the cavity are taken into account in the loss of the rear mirror), and, using Eqs. (1a) and (1b), it is possible to find a relation that connects the pump and the laser intensities. Then Γ reads as follows:

$$\Gamma = \sqrt{R_m R_s}^{-\frac{\alpha_0}{g_0}} \exp\{-\alpha_0(f_p - f_l)L\}. \tag{9}$$

The optimum length for which the laser wave is not reabsorbed leads to maximum output power. Then the pump transmission must be equal to β, leading to

$$L_{\text{opt}} = \frac{-1}{f_p - f_l}\ln\left\{\sqrt{R_m R_s}^{\frac{1}{g_0}}\beta^{\frac{1}{\alpha_0}}\right\}. \tag{10}$$

This result can also be obtained by computing the length for which $I_{\text{out}}(L)$ is maximum using Eq. (8). In continuous-wave laser operation of a three-level system, the inversion density of the gain media remains constant above the laser threshold. Then, for a given laser medium, the pump transmission is fixed and determined by the cavity loss level and spectroscopic parameters of the gain media. It is worth mentioning that L_{opt} as well as β depends on the pump intensity.

We now investigate the length and the ion concentration of the crystal for which oscillation at 1050 nm is preferred. The emission transitions of Yb:YAG are from upper level u_1 to lower level l_3(1030 nm) and l_4(1050 nm). First, as the l_4 energy level is higher than the l_3 level, its thermal population is lower and the f_l parameter at room temperature is 0.0284 versus 0.0646. Then the corresponding optimum crystal length is larger and more pump energy is absorbed. Using Eq. (10) we compute the optimum crystal length versus the rear mirror reflectivity for various pump intensities. The values of the crystal parameters used for the computation are listed in Table 1. The cross sections are spectroscopic [14].

Figure 2 shows the computed optimum lengths for the two wavelengths of 1030 and 1050 nm and for (a) 5 and (b) 10 at. % doping concentrations. We observed that, for a crystal length of 4 mm with 5 at. % doping, the crystal length is much lower than the optimum length for 1050 nm oscillation at different pump intensities but is close to the 1030 nm optimum length. As a result, oscillation at 1030 nm is preferred and shows good agreement with the results reported in [5]. In Ref. [5] a 5% doped, 3.5 mm long Yb:YAG crystal was used. Under the pump intensity of approximately 36 kW/cm^2, laser oscillation was achieved at the wavelength of 1030 nm. But, for the 10 at. % doped crystal, one can see that the situation is different. The preferred crystal length is much shorter than that of a 5 at. % doping crystal. Only when the crystal is very short, is oscillation at 1030 nm preferred. If the crystal length reaches a proper value, such as 4 mm, the 1030 nm laser is more likely to be reabsorbed and suppressed. This indicates a new way to suppress 1030 nm and obtain oscillation at 1050 nm only by choosing the Yb:YAG crystal with proper ion concentration and optimized length.

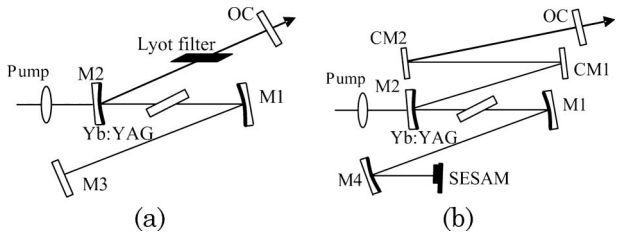

Fig. 3. Cavities used to study the (a) CW and (b) mode-locked laser performance of a Yb:YAG laser. M1, M2, M4, concave mirrors with a radius of curvature of 100 mm; M3, plane high reflector; CM1 and CM2, GTI mirrors; OC, output coupler.

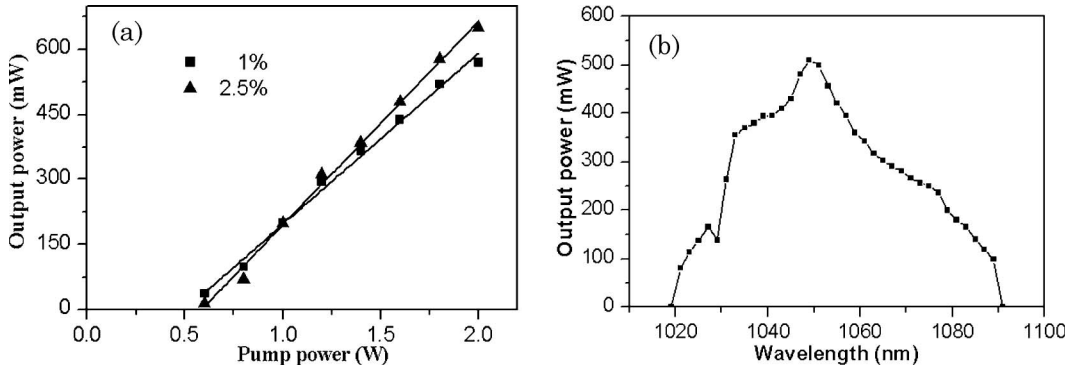

Fig. 4. (a) CW laser output power at 1050 nm versus the pump power and (b) the tuning curve with the 1% output coupler and with an incident pump power of 2 W.

3. Experiment

We performed the experiment with a 10 at. % doped Yb:YAG crystal having a length of 4 mm. A typical Z-shape cavity was used, and the crystal was located in the middle of two concave high reflectors (M1 and M2), each with a radius of curvature of 10 cm; see Fig. 3(a). All the coatings of the intracavity mirrors are identical for 1030 and 1050 nm. We used a continuous-wave Ti:sapphire laser at 940 nm as the pump. The maximum power available was 2 W. The pump beam was focused onto the crystal by a 100 mm focal length lens. The pump intensity at the front face of the Yb:YAG crystal is calculated to be approximately 43.7 kW/cm^2 at 2 W pump power. The measured absorption of the crystal to the pump light is 91%, which is in good agreement with the theoretically calculated value of 92.6% from Eq. (9).

For continuous-wave operation, we adopted two kinds of output coupler with transmittivities of 1% and 2.5%, respectively. Figure 4(a) shows the variation of the output power of the free-running laser as a function of pump power with different output couplers. The wavelength of the free-running laser was measured with a scanning spectrometer. When the pump power was increased from the threshold power to 2 W, the emitting wavelength was kept at 1050 nm. This can be well explained by Fig. 2(b). When the pump intensity was increased from zero to 43.7 kW/cm^2, the length of the crystal was near the optimum length of 1050 nm oscillation and much longer than that at 1030 nm oscillation. Lasing at 1030 nm is more likely to be reabsorbed and oscillation at the wavelength of 1050 nm is preferred. Under a pump power of 2 W, the maximum output power was as high as 650 mW, leading to a slope efficiency as high as 45.8%.

The laser tunability was studied by inserting a two-plate birefringent filter under Brewster angle, as shown in Fig. 3(a). Figure 4(b) shows the results obtained for $T_{OC} = 1\%$. The full tuning range extends continuously from 1021 to 1089 nm, with a FWHM of 44 nm. Based on the continuous-wave 1050 nm operation, we investigated the passive mode-locking operation of this laser. The cavity layout is shown in Fig. 3(b). The highly reflective rear mirror M3 was replaced by a piece of SESAM combined with a 100 mm radius-of-curvature concave mirror M4, which was used to reduce the incident beam size on the SESAM. The SESAM was designed for 0.4% modulation depth and a saturation fluence of 120 $\mu J/cm^2$ at the central wavelength of 1040 nm (BATOP GmbH, Jena, Germany). Considering the additional losses caused by the SESAM, we replaced the output coupler with a 0.5% coupler. Without intracavity dispersion compensation, we obtained stable mode-locked pulses in the picosecond regime. A typical intensity autocorrelation trace (obtained with an FR-103MN autocorrelator, Femtochrome Research, Berkeley, California) of the output pulses is shown

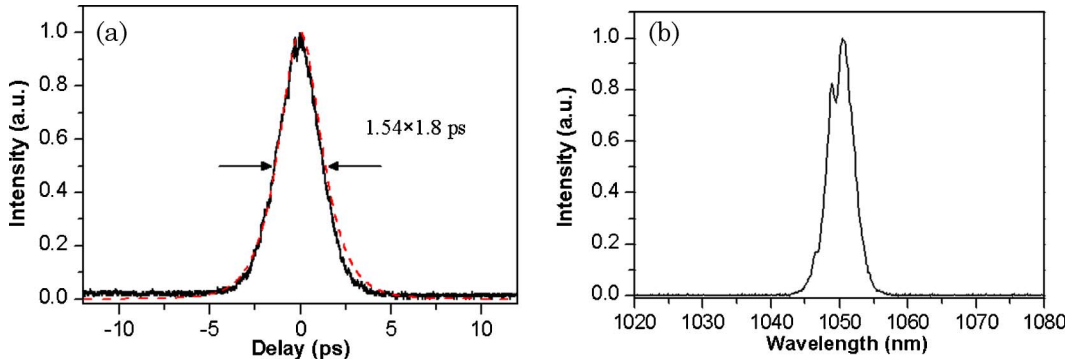

Fig. 5. (Color online) (a) Typical intensity autocorrelation trace of picosecond pulses and (b) the laser spectrum of picosecond operation.

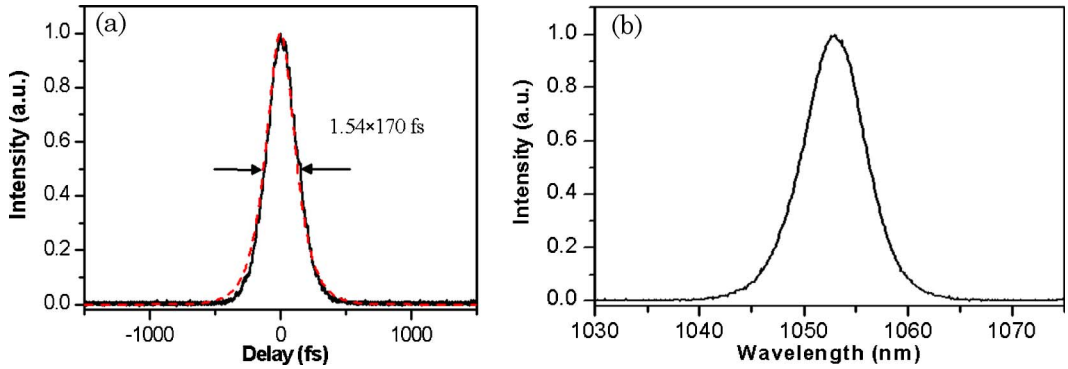

Fig. 6. (Color online) (a) Typical intensity autocorrelation trace of the femtosecond pulses and (b) the laser spectrum of femtosecond operation.

in Fig. 5(a). Assuming a sech^2 pulse shape, one can obtain the FWHM pulse duration of 1.8 ps. A simultaneous measurement of the pulse spectrum is illustrated in Fig. 5(b).

To obtain femtosecond pulses, we used a pair of Gires–Tournois interferometer (GTI) mirrors, which introduce group delay dispersion (GDD) of $-1200\ \mathrm{fs}^2$ from 1020 to 1080 nm by single pass. It is enough to compensate the positive GDD caused by the Yb:YAG crystal and the net intracavity GDD remains at a minus value. With this alignment, stable self-starting solitonlike pulses were obtained. Figure 6 shows the measured autocorrelation trace and the spectrum of the pulses. The pulse width is 170 fs assuming a sech^2 shape pulse, and the FWHM spectral bandwidth reaches 7 nm. The central wavelength redshifted from 1050 to 1053 nm. It is worth mentioning that the central wavelength of this femtosecond Yb:YAG laser is exactly the working wavelength of a high energy Nd:glass based ultrafast amplifier system. This experiment indicates that the femtosecond Yb:YAG laser has the potential to be an excellent seed source for the above system. Under the full pump power of 2 W, the average power of the femtosecond pulses is 180 mW at a repetition rate of 80 MHz, corresponding to the peak power of 13.3 kW.

4. Conclusion

In conclusion, we have described a novel method that combines numerical and experimental studies to suppress 1030 nm and obtain 1050 nm oscillation for the Yb:YAG laser. Numerical simulations were carried out to estimate the preferred emission wavelength of a continuous-wave Yb:YAG laser by taking into account the pump intensity, crystal length, and ion concentration. Then, by adopting the Yb:YAG crystal with proper length and ion concentration, we suppressed the 1030 nm oscillation and achieved efficient continuous-wave 1050 nm lasing, which is in fair agreement with the numerical model. On this basis, we demonstrated a femtosecond Yb:YAG laser at a central wavelength of 1053 nm, with a pulse width of 170 fs and a spectral bandwidth of 7 nm. We believe that the results of this study indicate a new way to obtain 1053 nm femtosecond pulses with a Yb:YAG laser. If we were to replace the pump laser with a diode laser at the same wavelength, even higher output power would be possible in a compact configuration. Because of the excellent properties of this crystal and its potential broad emission bandwidth at this wavelength, a 1053 nm femtosecond Yb:YAG laser with high power, high efficiency, and a short pulse width operation is hopeful, which will be one of the excellent seed sources for a high-nergy Nd:glass laser facility.

This research was partly supported by the National Natural Science Foundation of China (NSFC) under grants 60490281 and 60608003, the National Basic Research Program of China, 2007CB815104, and the National High-Tech Research and Development Program of China.

References

1. E. Innerhofer, T. Südmeyer, F. Brunner, R. Paschotta, and U. Keller, "Mode-locked high-power lasers and nonlinear optics: a powerful combination," Laser Phys. Lett. **1**, 82–85 (2004).
2. S. V. Marchese, C. R. E. Baer, A. G. Engqvist, S. Hashimoto, D. J. H. C. Maas, M. Golling, T. Südmeyer, and U. Keller, "Femtosecond thin disk laser oscillator with pulse energy beyond the 10-microjoule level," Opt. Express **16**, 6397–6407 (2008).
3. J. Neuhaus, J. Kleinbauer, A. Killi, S. Weiler, D. Sutter, and T. Dekorsy, "Passively mode-locked Yb:YAG thin-disk laser with pulse energies exceeding 13 μJ by use of an active multipass geometry," Opt. Lett. **33**, 726–728 (2008).
4. S. Uemura and K. Torizuka, "Kerr-lens mode-locked diode-pumped Yb:YAG laser with the transverse mode passively stabilized," Appl. Phys. Express **1**, 012007 (2008)
5. C. Hönninger, R. Paschotta, M. Graf, F. Morier-Genoud, G. Zhang, M. Moser, S. Biswal, J. Nees, A. Braun, G. A. Mourou, I. Johannsen, A. Giesen, W. Seeber, and U. Keller, "Ultrafast ytterbium-doped bulk lasers and laser amplifiers," Appl. Phys. B **69**, 3–17 (1999).
6. C. Hönninger, G. Zhang, U. Keller, and A. Giesen, "Femtosecond Yb:YAG laser using semiconductor saturable absorbers," Opt. Lett. **20**, 2402–2404 (1995).
7. M. Weitz, S. Reuter, R. Knappe, R. Wallenstein, and B. Henrich, "Passive mode-locked 21 W femtosecond Yb:YAG laser with 124 MHz repetition-rate," in *Technical Digest of Conference on Lasers and Electro-Optics* (Optical Society of America, 2004), paper CtuCC.

8. J. Aus der Au, G. J. Spühler, T. Südmeyer, R. Paschotta, R. Hövel, M. Moser, S. Erhard, M. Karszewski, A. Giesen, and U. Keller, "16.2 W average power from a diode-pumped femtosecond Yb:YAG thin disk laser, " Opt. Lett. **25**, 859–861 (2000).
9. S. Uemura and K. Torizuka, "Center-wavelength-shifted passively mode-locked diode-pumped ytterbium(Yb):yttrium aluminum garnet(YAG) laser," Jpn. J. Appl. Phys. **44**, L361–L363 (2005).
10. S. Magne, M. Druetta, J. P. Goure, J. C. Thevenin, P. Ferdinand, and G. Monnom, "An ytterbium-doped monomode fiber laser: amplified spontaneous emission, modeling of the gain and tenability in an external cavity," J. Lumin. **60–61**, 647–650 (1994).
11. H. M. Pask, R. J. Carman, D. C. Hanna, A. C. Tropper, C. J. Mackechnie, P. R. Barber, and J. M. Dawes, "Ytterbium-doped silica fiber lasers: versatile sources for the 1–1.2 μm region," IEEE J. Sel. Top. Quantum Electron. **1**, 2–13 (1995).
12. G. L. Bourdet, "Theoretical investigation of quasi-three-level longitudinally pumped continuous wave lasers," Appl. Opt. **39**, 966–971 (2000).
13. G. L. Bourdet and E. Bartnicki, "Generalized formula for continuous-wave end-pumped Yb-doped material amplifier gain and laser output power in various pumping configurations," Appl. Opt. **45**, 9203–9209 (2006).
14. R. J. Beach, "CW theory of quasi-three level end-pumped laser oscillators," Opt. Commun. **123**, 385–393 (1996).